JPET Fast Forward. Published on January 12, 2005 as DOI: 10.1124/jpet.104.081232

JPET#81232

Nicotinic receptor subtypes in rat hippocampal slices are differentially sensitive to desensitization and early *in vivo* functional upregulation by nicotine and to block by bupropion

Manickavasagom Alkondon and Edson X. Albuquerque

Department of Pharmacology and Experimental Therapeutics (M.A., E.X.A.) University of Maryland School of Medicine, Baltimore, MD 21201, USA; Departamento de Farmacologia Básica e Clínica (E.X.A.), Instituto de Ciências Biomédicas, Centro de Ciências da Saúde, Universidade Federal do Rio de Janeiro, Rio de Janeiro, RJ 21944, Brazil

Running title: Functional upregulation and desensitization of nAChRs

Corresponding author: Manickavasagom Alkondon (malko001@umaryland.edu), Department of Pharmacology and Experimental Therapeutics, University of Maryland School of Medicine, 655 W. Baltimore Street, Baltimore, MD 21201, USA. Tel: (410) 706-3563; Fax: (410) 706-3991

Number of text pages: 42

Number of tables: 2

Number of figures: 9

Number of references: 44

Number of words in the Abstract: 251

Number of words in the Introduction: 714

Number of words in the Discussion: 1502

List of Abbreviations:

ACSF, artificial cerebrospinal fluid; AMPA, α-amino-3-hydroxy-5-methyl-4-isoxazolepropionic acid; APV, DL-2-amino-5-phosphonovaleric acid; EC50, agonist concentration that elicits 50% of maximal effect; DHβE, dihydro-β-erythroidine; DMPP, 1,1-dimethy-4-phenylpiperazinium; EPSC, excitatory postsynaptic current; GABA, γ-amino butyric acid; HEPES, N-[2-hydroxyethyl]piperazine-N'-[2-ethane sulfonic acid]; IC50, antagonist concentration that blocks 50% of the agonist effect; nAChR, nicotinic acetylcholine receptor; NMDA, N-methyl-D-aspartate; SEM, standard error of the mean; SLM, stratum lacunosum moleculare; SR, stratum

radiatum

Recommended section: **Neuropharmacology**

Abstract

To identify the brain nicotinic acetylcholine receptor (nAChR) subtypes that may be involved in nicotine addiction, we investigated the actions of bupropion, a drug used in cigarette smoking cessation programs, and nicotine on three pharmacologically identified nAChRs in rat hippocampal slices namely Type IA, Type II and Type III nAChRs, likely representing α7, α4β2, and α3β4 subunits respectively. Using whole-cell patch-clamp recordings from interneurons of acute hippocampal slices prepared from male rat pups, we studied the effect of nicotine on *in vivo* upregulation and *in vitro* desensitization of nAChRs. Two subcutaneous injections of nicotine (0.586 mg/kg free base, in less than a day) to rats at postnatal days 14-15 significantly enhanced the magnitude of functional responses arising from Type III and Type II, but not Type IA nAChRs. This treatment did not increase the functional affinity for acetylcholine at Type II nAChRs. A single injection of nicotine also produced a significant increase in Type III nAChR response. In addition, Type III and Type II, but not Type IA nAChRs, are desensitized by *in vitro* exposure to nicotine at concentrations found in the venous blood of cigarette smokers. Bupropion at 1 μM produced 56%, 15% and 0% inhibition of Type III, Type II and Type IA nAChR responses, respectively, in the slices. Our results suggest that *in vivo*-nicotine-induced nAChR upregulation observed in neurons of intact brain tissue is a physiologically relevant phenomenon, and that early upregulation of Type III and Type II nAChRs could be an important biological signal in nicotine addiction.

The biological basis of nicotine addiction is attributed primarily to the actions of this tobacco alkaloid on various nicotinic acetylcholine receptor (nAChR) subtypes in the brain (Dani and Heinemann, 1996). Although the nAChR subunits β2 (Picciotto et al., 1998) and α4 (Tapper et al., 2004) have been implicated in the reinforcing properties of nicotine and β4 in the withdrawal effects of nicotine (Salas et al., 2004), the relative importance of each native brain nAChR subtype in nicotine addiction is still unknown. Among the various known actions of nicotine, nAChR upregulation is a well-documented observation, believed to play a central role in nicotine addiction (Buisson and Bertrand, 2002; Gentry and Lukas, 2002). Upregulation of nAChRs has been observed in human brain tissue of smokers (Breese et al., 1997), animal brain after a prolonged exposure to nicotine (Marks et al., 1992; Flores et al., 1992; Zhang et al., 1994; Rowell and Li, 1997; Nguyen et al., 2004), and to a greater extent in cell lines expressing different combinations of nAChR subunits (Peng et al., 1994, Fenster et al., 1999; Buisson and Bertrand, 2001; Gentry and Lukas, 2002). However, it is unclear whether the upregulation of nAChRs as determined by an increase in the number of binding sites is always functional and physiologically relevant because it represents mainly intracellular pools (Gentry and Lukas, 2002; Sallette et al., 2004). Considering that nAChRs present in different brain regions are the natural targets for the actions of nicotine and may also have different compositions than the receptors studied in artificial expression systems, a clear understanding of nicotine addiction requires a more vivid knowledge of the functional status of nAChRs present in brain tissue after *in vivo* nicotine exposure. However, with the exception of a handful of studies in which functional nAChR upregulation was directly evaluated in intact neurons using primary cultures (Almeida et al., 2000; Kawai and Berg, 2001; Nashmi et al., 2003), we are not aware of any

studies that investigated functional nAChR upregulation using identified neuron types present in intact brain tissue.

In view of such paucity of information and the fact that hippocampus contains multiple subtypes of nAChRs (Alkondon and Albuquerque, 2004) that are also present in other brain regions (Aramakis and Metherate, 1998; Zoli et al., 1998; Wooltorton et al., 2003) and are likely to be involved in nicotine addiction, we sought to evaluate the effects of exposure to *in vivo* and *in vitro* nicotine on three pharmacologically identified nAChR subtypes in the CA1 interneurons of rat hippocampal slices. The three subtypes in the hippocampal slices (Alkondon et al., 2003; Alkondon and Albuquerque, 2004) are referred here as Type IA, Type II and Type III nAChRs because they exhibit a pharmacological profile similar to that of the nAChRs in cultured hippocampal neurons (Albuquerque et al., 1997) and also in mouse brain slice neurons (Zoli et al., 1998). Evidence from several studies suggests that type IA nAChRs consist of α7 subunits, type II nAChRs consist of α4β2 subunits and type III nAChRs contain of at least α3β4 subunits (Albuquerque et al., 1997; Zoli et al., 1998; Alkondon et al., 2003). Here, we investigated the changes in the magnitude of nAChR responses after either two injections or a single injection of nicotine because an early effect of this alkaloid could signify the development of lasting cues associated with nicotine addiction as it is the case for other drugs of abuse in general (Saal et al., 2003). Further, we compared the desensitizing effects on various hippocampal nAChRs of acute *in vitro* nicotine exposure, because desensitization appears to be essential and often precedes receptor upregulation in other systems (Peng et al., 1994; Fenster et al., 1999). Finally, we tested the effects of bupropion on native nAChR subtypes in hippocampal slices because this drug, currently used in smoking cessation programs, has shown some degree of selectivity towards α3

subunit-containing nAChRs (Fryer and Lukas, 1999; Slemmer et al., 2000). In this study, we demonstrate that Type III and Type II nAChRs are sensitive to functional upregulation after *in vivo* nicotine, are desensitized by nicotine at concentrations similar to those found in cigarette smokers, and are blocked by bupropion at clinically relevant concentrations. Thus, our results support the notion that both Type III and Type II nAChRs play important roles in nicotine addiction.

Material and Methods

Hippocampal slices. Slices of 250-μm thickness were obtained from the hippocampus of 15–19-day-old Sprague-Dawley rats according to the procedure described earlier (Alkondon et al., 2003). Animal care and handling were done strictly in accordance with the guidelines set forth by the Animal Care Committee of the University of Maryland, Baltimore. Slices were stored at room temperature in artificial cerebrospinal fluid (ACSF), which was bubbled with 95% O_2 and 5% CO_2 and composed of (in mM): NaCl, 125; $NaHCO_3$, 25; KCl, 2.5; NaH_2PO_4, 1.25; $CaCl_2$, 2, $MgCl_2$, 1; and glucose, 25. Stratum radiatum (SR) and stratum lacunosum moleculare (SLM) interneurons in the CA1 field of the slices were visualized by means of infrared-assisted videomicroscopy. Additionally, biocytin labeling was used to identify the neurons morphologically (Alkondon et al., 2003).

In vivo nicotine injection. Male rat pups at postnatal days 14 or 15 were injected subcutaneously twice in less than 24 h with either saline or nicotine. The first injection was done at 4-5 PM, and the second at 8-9 AM next morning. Brains were collected for electrophysiological experiments 1 - 2 h after the second saline or nicotine injections. In another set of experiments, a single injection of saline or nicotine was given on postnatal day 15, and 17 hours later, experiments were conducted. Typically, two male rat pups from the same litter were used on the same day, one for saline and the other for nicotine. Nicotine hydrogen tartrate dissolved in sterile saline was injected at a dose of 3.6 μmol/kg (equivalent to 0.586 mg/kg free base) in a 10 ml/kg volume. A 10 min visual observation of the animal behavior after the injections revealed that there were occasional tremors and a slight increase in locomotor activity

in the nicotine-treated group.

Electrophysiological recordings. Excitatory postsynaptic currents (EPSCs) and agonist-evoked whole-cell currents were recorded from the soma of CA1 interneurons according to the standard patch-clamp technique using an LM-EPC7 amplifier (List Electronic, Darmstadt, FRG). Agonists were applied to the slices via a U-tube, and antagonists were applied both via the U-tube and bath perfusion (Alkondon et al., 2003). Signals were filtered at 2 kHz and either recorded on a video tape recorder for later analysis or directly sampled by a microcomputer using the pCLAMP 9 program (Axon Instruments, Foster City, CA). Neurons were superfused with ACSF at 2 ml/min. Atropine (1 μM) was added to the ACSF to block the muscarinic receptors. Bicuculline (10 μM) was added to ACSF to block $GABA_A$ receptor activity. Methyllycaconitine (MLA, 10 nM) was included in the ACSF while studying non-type IA nAChR responses. Patch pipettes were pulled from borosilicate glass capillary (1.2-mm outer diameter), and when filled with internal solution had resistance between 2 and 5 MΩ. The series resistance ranged from 8 to 20 MΩ. At −68 mV, the leak current was generally between 50 and 150 pA, and when it exceeded 200 pA, the data were not included in the analysis. The internal pipette solution contained 0.5% biocytin in addition to (in mM): ethylene-glycol bis(β-amino-ethyl ether)-N-N'-tetraacetic acid, 10; HEPES, 10; Cs-methane sulfonate, 130; CsCl, 10; $MgCl_2$, 2; and QX-314, 5 (pH adjusted to 7.3 with CsOH; 340 mOsm). Membrane potentials were corrected for liquid junction potentials. All experiments were carried out at room temperature (20−22^{o}C).

Data analysis. The frequency, peak amplitude, 10-90% rise time and decay-time constant of

AMPA EPSCs were analyzed using WinEDR V2.3 (Strathclyde Electrophysiology Software, Glasgow, Scotland). The peak amplitude of nicotinic currents and the net charge of NMDA receptor-mediated EPSCs and nicotinic currents were analyzed using the pCLAMP9 software (Axon Instruments, Foster City, CA). Typically, the net charge of agonist-evoked responses was calculated for the duration of the agonist pulse starting from the valve opening. Results are presented as mean ± SEM, and compared for their statistical significance by paired Student's t-test, Wilcoxon Signed Rank test or Mann-Whitney U test. Agonist concentration-response curves were fitted to a Hill equation, $I = (I_{max}*A^n)/(A^n+EC50^n)$, where I is the measured current amplitude or net charge, I_{max} is the maximum current amplitude or net charge, ^{n} is the Hill coefficient, EC50 is the agonist concentration producing half-maximal response.

Drugs used. ACh chloride, (-)bicuculline methiodide, bupropion hydrochloride, choline chloride, 1,1-dimethyl-4-phenylpiperazinium iodide (DMPP); (-)-nicotine hydrogen tartrate, DL-2-amino-5-phosphonovaleric acid (APV), lidocaine N-ethyl bromide (QX-314), NMDA, glycine, and atropine sulfate were obtained from Sigma Chemical Co. (St. Louis, MO). (±)Mecamylamine.HCl was a gift from Merck, Sharp & Dohme Research Laboratories (Rahway, NJ). Methyllycaconitine citrate (MLA) was a gift from Professor M.H. Benn (Dept. Chemistry, Univ. Calgary, Alberta, Canada). Stock solutions of all drugs were made in distilled water.

RESULTS

Two subcutaneous nicotine injections do not cause functional upregulation of Type IA nAChRs. Application of choline at 10 mM, a concentration that is nearly saturating, induced Type IA inward currents in CA1 SR interneurons at -68 mV (Fig. 1A). These currents decayed to the baseline before the end of agonist pulses. Such nicotinic currents, being sensitive to blockade by low concentrations of MLA and α-bungarotoxin (Albuquerque et al., 1997), represent the sole activation of α7 nAChRs in the SR interneurons. We compared the peak amplitude of functional Type IA nAChRs in these interneurons after two injections of rats with either saline or nicotine (3.6 μmol/kg, s.c in less than a day). The peak amplitude of choline-evoked Type IA currents, a measure of the activity of functional α7 nAChRs present in the somatodendritic regions of SR interneurons, ranged from 6 pA to 155 pA (n = 21 neurons) in saline-treated rats and from 6 pA to 432 pA (n = 24 neurons) in nicotine-treated rats (Fig. 1B). A statistical analysis of the data indicated that the mean values of the peak amplitude of choline-elicited currents are not significantly different ($p > 0.05$ by Mann Whitney test) between saline-injected and nicotine-injected rats (Fig. 1C). We also compared the differences between the two groups based on net charge of choline-evoked currents as the net charge of the currents is considered a better measure of receptor activity than the peak amplitude of the currents under conditions where solution exchange around the neuron is slow (Papke and Papke, 2002) as it would occur in the brain slices. Similarly to those observed in the peak amplitude analysis, the net charge of choline-evoked currents also showed an identical pattern between the two groups

of rats (Fig. 1B, 1C). Further, no significant differences between the two groups of animals were noted on the mean decay time constant of choline-induced currents (Fig. 1C). We conclude from the above results that two nicotine injections, at the dose used, are unable to functionally upregulate to any significant extent the activity of Type IA nAChRs and modify the properties of these receptors.

Two subcutaneous nicotine injections functionally upregulate Type II nAChRs. Application of ACh (1 mM) in the presence of MLA induced slowly decaying Type II inward currents at -68 mV in all the SLM interneurons (n = 42) and 25 % of SR interneurons (n = 40) tested. Such slowly decaying nicotinic currents, being sensitive to blockade by DHβE, poorly activated by cytisine, represent the activation of α4β2 nAChRs in the CA1 interneurons (Alkondon et al., 2000, 2003). In saline- and nicotine-treated rats, ACh (1 μM to 3 mM) evoked concentration-dependent increase in the current amplitude with higher values observed in the nicotine group (Fig. 2A). In saline-treated rats, the plot of the peak amplitude of the inward currents against ACh concentration yielded a single sigmoidal curve with an EC50 of 112 μM (Fig. 2B, Table 1). The plot of net charge of these currents against agonist concentration gave an EC50 of 117 μM (Fig. 2C; Table 1). In nicotine-treated rats, both peak amplitude and net charge of nicotinic currents were higher than in saline-treated rats at ACh concentration >1 μM, the differences were statistically significant ($p < 0.05$ by Mann-Whitney test) at several ACh concentrations between 10 μM and 3 mM (Fig. 2B, 2C; Table 1). On average, nicotine treatment caused about 2-fold increase in the net charge of ACh (1mM)-induced currents (Fig. 2C). In the nicotine group, the plot of the peak amplitude against concentration yielded an EC50 of 123 μM and that of net

charge against concentration gave an EC50 of 104 μM. The EC50 values between saline and nicotine groups were not significantly different (see Table 1) suggesting that the affinity for ACh was unchanged by nicotine treatment. We conclude from the above results that two nicotine injections cause significant functional upregulation of Type II nAChRs.

Two subcutaneous nicotine injections functionally upregulate Type III nAChRs. Our previous studies and that of Zoli et al (1998) have suggested that Type III nAChRs are represented by α3β4-like subunits, and activation of Type III nAChRs in the hippocampal slices induces vesicular glutamate release that was detected in CA1 SR interneurons by the appearance of EPSCs mediated via AMPA and NMDA receptors (Alkondon et al., 2003). Here, we determined the effect of two subcutaneous injections of nicotine on Type III nAChR responses by recording ACh-elicited AMPA EPSCs or NMDA EPSCs in SR interneurons.

At -68 mV, in the presence of $GABA_A$ receptor antagonist bicuculline, occasional spontaneous inward AMPA EPSCs were observed in the whole-cell recordings from SR interneurons at postnatal day 15 in saline-injected rats. Two *in vivo* nicotine injections caused a slight increase (but not significantly different from control, see Table 2) in the frequency of spontaneous AMPA EPSCs. In the saline-treated rats, U-tube application of ACh induced a marginal increase at 10 μM and a significant increase at 100 μM in the frequency of AMPA EPSCs (see Fig. 3 and Table 2). In the nicotine-injected rats, ACh at both 10 and 100 μM induced a larger increase in the frequency of AMPA EPSCs (Fig. 3, Table 2). The effect of both concentrations of ACh was significantly higher in the nicotine group compared to saline group (n = eight to nine neurons in each group; Table 2). Nicotine injections did not affect the rise time or

the decay time constant of ACh-evoked AMPA EPSCs (see Table 2). However, the peak amplitude of AMPA EPSCs evoked by 100 μM ACh was significantly higher in the nicotine group compared to saline control (Table 2). Further, these high-amplitude events were also associated with a slow NMDA component, particularly in the nicotine-treated group (see inset in Fig. 3).

To evaluate ACh-evoked NMDA EPSCs in greater detail, recordings were carried out at positive membrane potentials (+48 mV) to remove Mg^{2+}-block of NMDA channels. In saline-injected rats, 10 μM ACh evoked NMDA EPSCs in five out of seven neurons. Increasing the concentrations of ACh to 30 μM, 100 μM and 1000 μM produced proportionately larger magnitude NMDA EPSCs (Fig. 4A, 4B), suggesting a concentration-dependent activation of Type III nAChRs. On the other hand, in nicotine-injected rats, 10 μM ACh induced NMDA EPSCs in all nine interneurons tested. Higher concentrations of ACh induced much larger responses in nicotine-treated rats than in saline-treated rats (Fig. 4A, 4B). At each of the four ACh concentrations, the values of net charge of NMDA EPSCs obtained in the nicotine group were significantly higher than those in the saline group ($p < 0.02$; Mann-Whitney test). On average, nicotine treatment caused about 3-fold increase in the net charge of NMDA EPSCs induced by 1 mM ACh (Fig. 4B).

To rule out the possibility that nicotine-induced enhancement of net charge of ACh-evoked NMDA EPSCs resulted from an increase in the postsynaptic NMDA receptor responsiveness, we compared currents (Fig. 5A) evoked by U-tube application of NMDA to SR interneurons in both groups of animals. As illustrated in Fig. 5C, the net charge of NMDA-evoked currents in the CA1 SR interneurons did not reveal differences between saline- and

nicotine-treated rats. Further, if nicotine enhanced the net charge of ACh-evoked NMDA EPSCs by increasing the number of glutamate synapses on the dendrites, then one should expect that activation of glutamate synapses via a non-nicotinic mechanism would also produce enhanced responses after nicotine treatment. To verify this possibility, we activated glutamate synapses by applying 500 mM sucrose, a hyperosmotic solution known to induce transmitter release from the terminals in a Ca^{2+}-independent manner (Rosenmund and Stevens, 1996). U-tube applied sucrose induced an outward current at +40 mV that resulted from the summation of several NMDA EPSCs because bath-applied APV (50 μM) attenuated the response dramatically (Fig. 5B). However, the magnitude of sucrose-evoked currents remained same in both groups of animals (Fig. 5B, 5C), indicating that nicotine's effect on NMDA EPSCs did not arise from a change in the number of glutamate synapses. We conclude from the above results that two nicotine injections functionally upregulate Type III nAChRs to a significant extent.

Single subcutaneous nicotine injection functionally upregulates Type III nAChRs. Next, we tested the effect of single injection of nicotine on the functional upregulation. In this protocol, a single injection of saline or nicotine (3.6 μmol/kg, s.c) was given to rats on postnatal day 15 and experiments conducted 17 hours later on day 16. DMPP, another nicotinic agonist, was used to activate the NMDA EPSCs in the presence of 10 nM MLA. As illustrated in Fig. 6A, DMPP induced NMDA EPSCs in SR interneurons from both groups of rats; however, the magnitude of the response was larger in the nicotine-treated rats. Analysis of the net charge of DMPP-evoked NMDA EPSCs revealed a significant increase in the values in the nicotine group; about 2.7 fold that of saline-treated rats (Fig. 6B). These results indicated that single injection of

nicotine is as effective as two injections with respect to upregulation of Type III nAChRs. Further, as the agonist DMPP is not hydrolyzed by acetylcholinesterase, these experiments ruled out any changes in acetylcholinesterase activity as an explanation for increased ACh response after *in vivo* nicotine injections in the above-mentioned experiments.

In another set of experiments, we tested the pharmacological sensitivity of Type III nAChR in control and nicotine-injected rats to find out whether *in vivo* nicotine exposure altered the properties of these receptors. We have shown previously that 1 μM mecamylamine inhibits about 80% of Type III nAChR response in control rats (Alkondon et al., 2003). Here, in nicotine-injected rats (one injection, 17 h) 1 μM mecamylamine induced a mean inhibition of about 83% (n=6 neurons) of the Type III nAChR response, a value not significantly different between control and nicotine-injected rats (Fig. 7). Our previous study also revealed that MLA at 10 nM, a concentration known to inhibit α7 nAChR-mediated currents, failed to affect the Type III nAChR response (Alkondon et al., 2003). Here, we tested the effect of MLA at 50 nM, a concentration found to inhibit α6-containing nAChRs in the rat striatum (Mogg et al., 2002). We observed that 50 nM MLA produced about 30% (n=6) and 26% (n =6) inhibition of Type III nAChR in control and nicotine-injected rats, respectively. There were no significant differences between control and nicotine-injected rats in the magnitude of inhibition by MLA (Fig. 7). These results suggest that there is no major alteration in the pharmacological sensitivity of Type III nAChR after *in vivo* nicotine injections.

In vitro nicotine exposure differentially desensitizes three nAChRs in the hippocampal slices. Receptor desensitization has been linked to receptor upregulation in several *in vitro*

model systems (Peng et al., 1994; Fenster et al., 1999; Buisson and Bertrand, 2001). This raises the possibility that variable degree of desensitization could account for the observed differences in the upregulation of hippocampal nAChRs by nicotine injections. To test this hypothesis, we studied the concentration dependence for nicotine to induce *in vitro* desensitization of three nAChR subtypes in the hippocampal slices. Nicotine-induced desensitization of Type III nAChRs was assessed from inhibition of ACh (100 μM)-evoked NMDA EPSCs recorded from CA1 SR interneurons. A 10 min exposure of the slices to nicotine (1 to 100 nM) caused a concentration-dependent inhibition of ACh (100 μM)-evoked NMDA EPSCs (Fig. 8B). At 100 nM nicotine, ACh-evoked NMDA EPSCs were completely abolished (see Fig. 8A). The plot of the net charge of ACh-evoked NMDA EPSCs versus concentration of nicotine yielded an IC50 of 12.8 ± 0.1 nM and a Hill coefficient of 1.97 ± 0.02 for inhibiting Type III nAChR responses (Fig. 8B). Nicotine-induced desensitization of Type II nAChRs was assessed from inhibition of ACh (100 μM)-evoked slow inward currents recorded from SLM interneurons in the continuous presence of MLA (10 nM). A 10 min exposure of the slices to nicotine (10 to 500 nM) inhibited in a concentration-dependent manner ACh-evoked slow inward currents (Fig. 8B). At 100 nM nicotine, there was only partial inhibition of ACh-evoked currents seen (Fig. 8A). Although nicotine at 500 nM produced substantial inhibition, nearly 15% of the currents still remained (Fig. 8B). The plot of the net charge of ACh-evoked slow inward currents versus concentration of nicotine yielded an IC50 of 124 ± 17 nM and a Hill coefficient of 1.33 ± 0.19 for inhibiting Type II nAChR-mediated currents (Fig. 8B). Nicotine-induced desensitization of Type IA nAChRs was assessed from inhibition of choline (10 mM)-evoked inward currents recorded from CA1 SR interneurons. Data from a previous study on Type IA nAChRs (Alkondon et al., 2000)

was used here for comparison with other subtypes. A 10 min exposure of the slices to nicotine (100 to 2500 nM) inhibited in a concentration-dependent manner choline-evoked inward currents (Fig. 8B). At 100 nM nicotine, there was practically no inhibition observed (Fig. 8A). The plot of the peak amplitude of choline-evoked inward currents versus concentration of nicotine yielded an IC50 of 653 ± 26 nM and a Hill coefficient of 2.78 ± 0.26 for inhibiting Type IA nAChRs (Fig. 8B).

In vitro exposure to bupropion potently inhibits Type III nAChR-mediated NMDA EPSCs. From the above results it is evident that Type III nAChRs are a sensitive target for the *in vivo* and *in vitro* actions of nicotine. Therefore, one can predict that blockade of this native subtype could be beneficial to some extent in nicotine dependence and addiction. To verify this, we tested the effects of a well-known anti-smoking agent, bupropion, on ACh-elicited NMDA EPSCs. A 10 min bath application of bupropion (1 μM) attenuated ACh-induced NMDA EPSCs (Fig. 9A). The inhibitory effect was completely reversible within 20 min wash with drug-free ACSF. On average, there was about 56 % inhibition with 1 μM (n = 6) bupropion. The effect at 1 μM was statistically significant ($p < 0.01$ by Student's paired *t* test). At 1 μM, bupropion produced marginal but significant ($p < 0.05$ by paired '*t*' test) inhibition of Type II nAChR-mediated currents (Fig. 9B, 9E), but did not alter currents originating from either Type IA nAChRs (Fig. 9C, 9E) or NMDA receptors (Fig. 9D, 9E). The degree of blockade induced by 1 μM bupropion at Type III, Type II and Type IA nAChRs (see Fig. 9) is comparable to that observed for α3β4, α4β2 and α7 nAChRs studied in artificial expression systems (Fryer and Lukas, 1999; Slemmer et al., 2000).

DISCUSSION

The present results disclosed major differences in the susceptibility of three distinct brain nAChR subtypes to the *in vivo* and *in vitro* actions of nicotine and to the blocking effects of bupropion. By evaluating the activity of nAChRs, this study, for the first time, demonstrated the propensity of *in vivo* nicotine to functionally upregulate nAChRs in identified neuron types present in intact brain tissue.

Functional upregulation by *in vivo* nicotine. The main finding of this study is that nicotine injections in less than a day is able to functionally upregulate type III and type II, but not type IA nAChRs in the hippocampal slices. Both type IA and type II nAChRs were evaluated directly by studying the receptor-mediated currents, whereas type III nAChR activity was assessed indirectly via ACh-evoked glutamate EPSCs. Although the indirect measurement of type III nAChRs is a limitation in this study, multiple lines of evidence prove that upregulation by nicotine takes place at the type III nAChRs only. Firstly, the net charge of ACh-induced NMDA EPSCs increased as a function of ACh concentration as would be predicted for responses due to agonist-receptor interaction. Secondly, enhancement by *in vivo* nicotine could be seen at both AMPA EPSCs (Fig. 3) and NMDA EPSCs (Fig. 4), reflecting enhanced release of glutamate from the terminals and not enhanced sensitivity of postsynaptic NMDA receptors (see Fig. 5). These results support that nicotine-induced enhancement of glutamate EPSCs is a direct consequence of upregulation in the number and/or the activity of type III nAChRs present at the glutamate neurons or terminals.

Our results on type II nAChR functional upregulation by nicotine injection contrast with

the results of another study (Nguyen et al., 2004) in which the authors find no significant increase in α4β2 nAChR function after a 16 h nicotine exposure via osmotic pumps. It is possible that either methodological differences (such as injection versus osmotic pump or young versus adult rats) or heterogeneity of native nAChR subtypes could account for the observed differences in the two studies.

In vitro desensitization correlates with in vivo nAChR functional upregulation. A striking difference in the concentrations of nicotine for *in vitro* desensitization of hippocampal nAChRs (see Fig. 8B) validates our previous assumption that three pharmacologically classified nAChR subtypes are indeed separate structural entities. Comparison of nicotine's IC50s (Fig. 8B) indicated that Type III nAChRs are the most sensitive, Type II nAChRs being moderately sensitive, and Type IA nAChRs being the least sensitive for the desensitizing action of nicotine. Interestingly, comparison of the magnitude of nAChR functional upregulation by nicotine indicated a three-fold increase for Type III nAChRs, two-fold increase for Type II nAChRs and no significant increase for Type IA nAChRs (Figs 1, 2, 4), suggesting an inverse relationship between desensitization IC50 and percent upregulation. If this trend holds true for a wider *in vivo* nicotine doses, it can be predicted that a dose lower than 0.586 mg/kg free base of nicotine could functionally upregulate only Type III nAChRs. On the contrary, doses higher than 0.586 mg/kg and given for many days could functionally upregulate even Type IA nAChRs. In fact, our preliminary studies revealed that eight and 15 injections (4 and 8 days treatment), but not two injections of nicotine (0.586 mg/kg) induce significant functional upregulation of Type IA nAChRs when assessed from choline-induced GABAergic postsynaptic currents in SR

interneurons, a measure of Type IA nAChR activity in population of interneurons (Alkondon and Albuquerque, 2004).

Subunit make-up of the type III nAChR that modulates glutamate release onto the interneuron. Previous pharmacological analyses based on cytisine's efficacy for activation and mecamylamine's potency for blockade suggested that the nAChRs that modulate glutamate release onto the SR interneurons may be composed of a minimum of α3 and β4 subunits (Alkondon et al., 2003). The partial block of Type III nAChR response by 50 nM MLA (see Fig. 7) rules out the involvement of α6 subunits because this concentration of MLA is known to block α6-containing nAChRs in the rat striatum (Mogg et al., 2002). The high potency blockade by bupropion of ACh-induced NMDA EPSCs (see Fig. 9) further validates the involvement of α3 subunit in this nAChR because previous studies have shown that α3-containing nAChRs are the most sensitive subtype for the blocking action of bupropion (Fryer and Lukas, 1999; Slemmer et al., 2000). A recent study demonstrating that bupropion inhibits potently nicotine-evoked norepinephrine release from hippocampal slices via its action on α3β4-like nAChRs also supports this conclusion (Miller et al., 2002). Other reports that some somatic signs of nicotine withdrawal in mice depend on β4-containing nAChRs (Salas et al., 2004) and that bupropion reverses the expression of somatic aspects of nicotine withdrawal syndrome in rats (Cryan et al., 2003) are in line with our results. However, in most studies in artificial cell systems, α3β4 nAChRs are not potently desensitized or upregulated by nicotine (Fenster *et al.*, 1997; Wang *et al.*, 1998; Meyer *et al.*, 2001; Sallette *et al.*, 2004). Also, in the adult rats, chronic nicotine treatment for 2 weeks via osmotic pump fails to increase α3β4 nAChR function in the medial

habenula and interpeduncular nucleus as assessed by cytisine-induced rubidium efflux (Nguyen et al., 2004). It is possible that Type III nAChRs investigated in the hippocampal region of young postnatal rats (this study) are structurally and functionally distinct from the α3β4-like nAChR studied in the habenula region of adult rats (Nguyen et al., 2004). More detailed analysis may be required to assess the exact subunit composition of the type III nAChRs in neurons in order to understand its unique sensitivity to desensitization and upregulation.

Level of upregulation in cigarette smoking. The concentration of nicotine in the blood of a smoker fluctuates depending on several factors. The mean arterial blood levels, which reflects the brain concentrations, range from 37 to 58 ng/ml (equivalent to 228 to 357 nM) when measured within one min after end of smoking a single cigarette, and individual values reaching up to 92.5 ng/ml (i.e., 570 nM) (Henningfield et al., 1993). The concentration of nicotine in the venous blood varies between 5 and 30 ng/ml after smoking a single cigarette, but rises to 10 and 50 ng/ml after smoking several cigarettes (see Benowitz and Jacob, 1998). A plasma half-life of 2 hours in humans (Benowitz and Jacob, 1998) allows the venous concentration to build gradually and to remain in the blood stream for several hours, providing a condition in which the nAChRs in brain neurons can be desensitized and upregulated. The results portrayed in Fig. 8 indicate that Type III nAChRs will be desensitized completely, Type II nAChRs will be desensitized significantly, and Type IA nAChRs being spared from desensitization at the venous range of nicotine levels in cigarette smokers. Therefore, it is possible that in cigarette smokers, both Type III and Type II nAChRs are upregulated at a time when the Type IA nAChRs remain unaffected by the available nicotine concentrations, and such upregulated nAChRs may

contribute to altered neurotransmission in the brain of smokers.

Significance of bupropion blockade and early nicotine-induced upregulation of Type III nAChRs. The present results indicated that Type III nAChRs are the first among the three identified subtypes in the hippocampus to be readily desensitized by smoker's level of nicotine, significantly upregulated by *in vivo* nicotine in less than a day, and potently blocked by clinically relevant concentrations of bupropion (Fryer and Lukas, 1999; Slemmer et al., 2000). It is unlikely that a high-potency inhibition of Type III response by bupropion is due to measurement of an indirect rather than a direct response because the magnitude of the indirect response was directly proportional to the agonist concentrations (see Fig. 4). The Type III nAChRs when activated by exogenously applied agonists triggers both AMPA receptor- and NMDA receptor-mediated EPSCs (see Figs. 3 and 4) and thereby forms one of the means by which endogenous cholinergic impulse could regulate the excitability of interneurons (Alkondon et al., 2003). ACh-induced excitation of GABAergic interneurons is an important signal that improves attention and encoding by suppression of background activity in the cortical circuits (Hasselmo and McGaughy, 2004). It has been established that the activity of GABAergic interneurons is critical in setting up various hippocampal rhythms, indicative of the process of learning and memory (Cobb et al., 1999). As a single injection of nicotine is able to induce rapid synaptic changes that underlies cue-related learning (Saal et al., 2003) and is also able to functionally upregulate the nAChRs (see Fig. 6), we propose that early upregulation of Type III nAChRs by nicotine may be a key mechanism involved in early cue-related learning associated with nicotine addiction. It is also likely that blockade of upregulated Type III and Type II nAChRs remains one of the key

mechanisms by which bupropion produces beneficial effects in anti-smoking therapies. This is also consistent with the reports that bupropion and other α3β4 nAChR antagonists are able to suppress nicotine self administration in rats (Glick et al., 2002; Bruijnzeel and Markou, 2003; Rauhut et al., 2003).

Acknowledgements: The technical assistance of Barbara Marrow and Mabel Zelle is gratefully acknowledged. We are thankful to Bhagavathy Alkondon for excellent technical assistance in the preparation of hippocampal slices.

REFERENCES

Albuquerque EX, Alkondon M, Pereira EFR, Castro NG, Schrattenholz A, Barbosa CTF, Bonfante-Cabarcas R, Aracava Y, Eisenberg HM, and Maelicke A (1997) Properties of neuronal nicotinic acetylcholine receptors: pharmacological characterization and modulation of synaptic function. *J Pharmacol Exp Ther* **280:** 1117-1136.

Alkondon M and Albuquerque EX (2004) The nicotinic acetylcholine receptor subtypes and their function in the hippocampus and cerebral cortex. *Prog Brain Res* **145:** 109-120.

Alkondon M, Pereira EFR, Almeida LEF, Randall WR, and Albuquerque EX (2000) Nicotine at concentrations found in cigarette smokers activates and desensitizes nicotinic acetylcholine receptors in CA1 interneurons of rat hippocampus. *Neuropharmacol* **39:** 2726-2739.

Alkondon M, Pereira EFR, and Albuquerque EX (2003) NMDA and AMPA receptors contribute to the nicotinic cholinergic excitation of CA1 interneurons in the rat hippocampus. *J Neurophysiol* **90:** 1613-1625.

Almeida LEF, Pereira EFR, Alkondon M, Fawcett WP, Randall WR, and Albuquerque EX (2000) The opioid antagonist naltrexone inhibits activity and alters expression of α7 and α4β2 nicotinic receptors in hippocampal neurons: implications for smoking cessation programs. *Neuropharmacol* **39:** 2740-2755.

Aramakis VB and Metherate R (1998) Nicotine selectively enhances NMDA receptor-mediated synaptic transmission during postnatal development in sensory neocortex. *J Neurosci* **18:** 8485-8495.

Benowitz NL and Jacob III P (1998) Pharmacokinetics and metabolism of nicotine and related alkaloids. In: Arneric SP, Brioni JD (eds). *Neuronal nicotinic receptors: pharmacology and therapeutic opportunities.* Wiley-Liss, Inc. New York. pp 213-234.

Breese CR, Marks MJ, Logel J, Adams CE, Sullivan B, Collins AC, and Leonard S (1997) Effects of smoking history on [^{3}H]nicotine binding in human postmortem brain. *J Pharmacol Exp Ther* **282:** 7-13.

Bruijnzeel AW and Markou A (2003) Characterization of the effects of bupropion on the reinforcing properties of nicotine and food in rats. *Synapse* **50:** 20-28.

Buisson B and Bertrand D (2001) Chronic exposure to nicotine upregulates the human α4β2 nicotinic acetylcholine receptor function. *J Neurosci* **21:** 1819-1829.

Buisson B and Bertrand D (2002) Nicotine addiction: the possible role of functional upregulation. *Trends Pharmacol Sci* **23:** 130-136.

Cobb SR, Bulters DO, Suchak S, Riedel G, Morris RG, and Davies CH (1999) Activation of nicotinic acetylcholine receptors patterns network activity in the rodent hippocampus. *J Physiol* (Lond) **518:** 131-140.

Cryan JF, Bruijnzeel AW, Skjei KL, and Markou A (2003) Bupropion enhances brain reward function and reverses the affective and somatic aspects of nicotine withdrawal in the rat. *Psychopharmacology* **168:** 347-358.

Dani JA and Heinemann S (1996) Molecular and cellular aspects of nicotine abuse. *Neuron* **16:** 905-908.

Fenster CP, Rains MF, NoeragerB, Quick MW, and Lester RAJ (1997) Influence of subunit composition on desensitization of neuronal acetylcholine receptors at low concentrations of nicotine. *J Neurosci* **17:** 5747-5759.

Fenster CP, Whitworth TL, Sheffield EB, Quick MW, and Lester RAJ (1999) Upregulation of surface α4β2 nicotinic receptors is initiated by receptor desensitization after chronic exposure to nicotine. *J Neurosci* **19:** 4804-4814.

Flores CM, Rogers SW, Pabreza LA, Wolfe BB, and Kellar KJ (1992) A subtype of nicotinic cholinergic receptor in rat brain is composed of α4 and β2 subunits and is up-regulated by chronic nicotine treatment. *Mol Pharmacol* **41:** 31-37.

Fryer JD and Lukas RJ (1999) Noncompetitive functional inhibition at diverse, human nicotinic acetylcholine receptor subtypes by bupropion, phencyclidine, and ibogaine. *J Pharmacol Exp Ther* **288:** 88-92.

Gentry CL and Lukas RJ (2002) Regulation of nicotinic acetylcholine receptor numbers and function by chronic nicotine exposure. *Cur Drug Targets-CNS & Neurological Disorders* **1:** 381-407.

Glick SD, Maisonneuve IM, and Kitchen BA (2002) Modulation of nicotine self-administration in rats by combination therapy with agents blocking α3β4 nicotinic receptors. *Eur J Pharmacol* **448:** 185-191.

Hasselmo ME and McGaughy J (2004) High acetylcholine levels set circuit dynamics for attention and encoding and low acetylcholine levels set dynamics for consolidation. *Prog Brain Res* **145:** 207-231.

Henningfield JE, Stapleton JM, Benowitz NL, Grayson RF, and London ED (1993) Higher levels of nicotine in arterial than in venous blood after cigarette smoking. *Drug Alcohol Depen* **33:** 23-29.

Kawai H and Berg DK (2001) Nicotinic acetylcholine receptors containing alpha 7 subunits on rat cortical neurons do not undergo long-lasting inactivation even when up-regulated by chronic nicotine exposure. *J Neurochem* **78:** 1367-1378.

Marks MJ, Pauly JR, Gross SD, Deneris ES, Hermans-Borgmeyer I, Heinemann SF, and Collins AC (1992) Nicotine binding and nicotinic receptor subunit RNA after chronic nicotine treatment. *J Neurosci* **12:** 2765-2784.

Meyer EL, Xiao Y, and Kellar KJ (2001) Agonist regulation of rat α3β4 nicotinic acetylcholine receptors stably expressed in human embryonic kidney 293 cells. *Mol Pharmacol* **60:** 568-576.

Miller DK, Sumithran SP, and Dwoskin LP (2002) Bupropion inhibits nicotine-evoked [^{3}H] overflow from rat striatal slices preloaded with [^{3}H]dopamine and from rat hippocampal slices preloaded with [^{3}H]norepinephrine. *J Pharmacol Exp Ther* **302:** 1113-1122.

Mogg AJ, Whiteaker P, McIntosh JM, Marks M, Collins AC, Wonnacott S (2002) Methyllycaconitine is a potent antagonist of alpha-conotoxin-MII-sensitive presynaptic nicotinic acetylcholine receptors in rat striatum. *J Pharmacol Exp Ther* **302:** 197-204.

Nashmi R, Dickinson ME, McKinney S, Jareb M, Labarca C, Fraser SE, and Lester HA (2003) Assembly of α4β2 nicotinic acetylcholine receptors assessed with functional fluorescently

labeled subunits: effects of localization, trafficking, and nicotine-induced upregulation in clonal mammalian cells and in cultured midbrain neurons. *J Neurosci* **23:** 11554-11567.

Nguyen HN, Rasmussen BA, Perry DC (2004) Binding and functional activity of nicotinic cholinergic receptors in selected rat brain regions are increased following long-term but not short-term nicotine treatment. *J Neurochem* **90**: 40-49.

Papke RL and Papke JKP (2002) Comparative pharmacology of rat and human α7 nAChR conducted with net charge analysis. *Br J Pharmacol* **137:** 49-61.

Peng X, Gerzanich V, Anand R, Whiting PJ, and Lindstrom J (1994) Nicotine-induced increase in neuronal nicotinic receptors results from a decrease in the rate of receptor turnover. *Mol Pharmacol* **46:** 523-530.

Picciotto MR, Zoli M, Rimondini R, Lena C, Marubio LM, Pich EM, Fuxe K, and Changeux JP (1998) Acetylcholine receptors containing the beta2 subunit are involved in the reinforcing properties of nicotine. *Nature* **391:** 173-177.

Rauhut AS, Neugebauer N, Dwoskin LP, and Bardo MT (2003) Effect of bupropion on nicotine self-administration in rats. *Psychopharmacology* **169:** 1-9.

Rosenmund C and Stevens CF (1996) Definition of the readily releasable pool of vesicles at hippocampal synapses. *Neuron* **16:** 1197-1207.

Rowell PP and Li M (1997) Dose-response relationship for nicotine-induced up-regulation of rat brain nicotinic receptors. *J Neurochem* **68:** 1982-1989.

Saal D, Dong Y, Bonci A, and Malenka RC (2003) Drugs of abuse and stress trigger a common synaptic adaptation in dopamine neurons. *Neuron* **37:** 577-582.

Salas R, Pieri F, and De Biasi M (2004) Decreased signs of nicotine withdrawal in mice null for the β4 nicotinic acetylcholine receptor subunit. *J Neurosci* **24:** 10035-10039.

Sallette J, Bohler S, Benoit P, Soudant M, Pons S, Le Novère N, Changeux JP, and Corringer PJ (2004) An extracellular protein microdomain controls up-regulation of neuronal nicotinic acetylcholine receptors by nicotine. *J Biol Chem* **279:** 18767-18775.

Slemmer JE, Martin BR, and Damaj MI (2000) Bupropion is a nicotinic antagonist. *J Pharmacol Exp Ther* **295:** 321-327.

Tapper AR, KcKinney SL, Nashmi R, Schwarz J, Deshpande P, Labarca C, Whiteaker P, Marks MJ, Collins AC, Lester HA (2004) Nicotine activation of α4* receptors: sufficient for reward, tolerance, and sensitization. *Science* **306:** 1029-1032.

Wang F, Nelson ME, Kuryatov A, Olale, F, Cooper J, Keyser K, and Lindstrom J (1998) Chronic nicotine treatment up-regulates human alpha3 beta2 but not alpha3 beta4 acetylcholine receptors stably transfected in human embryonic kidney cells. *J Biol Chem* **273:** 28721-28732.

Wooltorton JRA, Pidoplichko VI, Broide RS, and Dani JA (2003) Differential desensitization and distribution of nicotinic acetylcholine receptor subtypes in midbrain dopamine areas. *J Neurosci* **23:** 3176-3185.

Zhang X, Gong ZH, and Nordberg A (1994) Effects of chronic nicotine treatment with (+)- and (−)-nicotine on nicotinic acetylcholine receptors and N-methyl-D-aspartate receptors in rat brain. *Br Res* **644:** 32-39.

Zoli M, Léna C, Picciotto MR, and Changeux JP (1998) Identification of four classes of brain nicotinic receptors using β2 mutant mice. *J Neurosci* **18:** 4461-4472.

Footnotes

This work was supported by the United States Public Health Service Grants NS41671 (EXA) and University of Medicine School of Medicine OTRD (EXA).

Figure Legends:

Fig. 1. Two in vivo nicotine injections do not affect expression of functional Type IA nAChRs.

A. Samples of choline-activated nicotinic inward currents, representing activation of Type IA nAChRs, recorded from CA1 SR interneurons. Samples portray low- and high-amplitude nicotinic currents observed in this study. Choline was applied to somatodendritic regions of interneurons via a U-tube for 12 sec (solid bar at the top of traces). Membrane Potential = -68 mV. ACSF contained 1 μM atropine and 10 μM bicuculline to inhibit muscarinic and $GABA_A$ receptors, respectively, in experiments described here and in other figures. Hippocampal slices were obtained from rats at postnatal days 15 or 16 after two subcutaneous injections of either saline or nicotine (0.586 mg/kg, free base) starting on day 14 or 15. **B**. Scatter plots of peak amplitude or net charge of choline-activated nicotinic inward currents from SR interneurons of hippocampal slices from saline- or nicotine-injected rats. n = 21 neurons in saline and 24 neurons in nicotine group. **C**. Plots of the mean and SEM values of peak amplitude, net charge and decay-time constant of nicotinic inward currents activated by choline from both groups of rats. No statistically significant differences in the mean values between saline and nicotine groups were found by Mann-Whitney test.

Fig. 2. Two in vivo nicotine injections enhance expression of functional Type II nAChRs.

A. Samples of ACh-activated slow-decaying nicotinic inward currents, representing activation of Type II nAChRs, recorded from CA1 SLM interneurons. Membrane Potential = -68 mV. MLA (10 nM) was also included in the ACSF to inhibit Type IA nAChRs. Different concentrations of ACh were applied via a U-tube. A 12-sec pulse of the agonist was applied at

an interval of about 8 min to allow for complete recovery from any desensitization from a previous agonist pulse. **B.** Plots of ACh concentrations versus peak amplitude of slow nicotinic currents. **C**. Plots of ACh concentrations versus net charge of slow nicotinic currents. Each symbol and error bar represent mean and SEM values obtained from four to ten neurons. Saline and nicotine injections were done by the same protocol as described in figure legend 1. Lines connecting the symbols represent fit of the mean values to a Hill equation. The values of peak amplitude and net charge were significantly different ($p < 0.05$ at 10, 30 and 3000 μM; $p < 0.02$ at 100 and 1000 μM) between the saline and nicotine group by Mann-Whitney U test.

Fig. 3. Two in vivo nicotine injections enhance expression of functional Type III nAChRs – Analysis of ACh-evoked AMPA EPSCs. Samples of ACh-evoked AMPA EPSCs, representing activation of Type III nAChRs, recorded from CA1 SR interneurons. Four lines of traces shown in each panel represent continuous whole-cell recording for 40 secs in each neuron. ACh (10 or 100 μM) was applied from the U-tube for the duration indicated by two thick vertical bars in the traces. Membrane potential = -68 mV. MLA (10 nM) was included in the ACSF to inhibit Type IA nAChRs. Note that ACh induces a concentration-dependent increase in the frequency of AMPA EPSCs in both the saline and the nicotine groups. Also, the ACh-induced effect is more prominent in the nicotine-treated rats than in the saline-treated rats. The insets on the right side of each panel represent selected EPSCs (indicated by asterisks on top of traces) shown on an expanded scale. Note the appearance of a slow NMDA component in the EPSCs in the nicotine group. Horizontal time scale = 2 s for main panel and 80 ms for insets.

Fig. 4. Two in vivo nicotine injections enhance expression of functional Type III nAChRs – Analysis of ACh-evoked NMDA EPSCs. **A**. Samples of ACh-evoked NMDA EPSCs, representing activation of Type III nAChRs, recorded from CA1 SR interneurons. Membrane Potential = +40 mV. MLA (10 nM) was included in the ACSF to inhibit Type IA nAChRs. Different concentrations of ACh were applied via a U-tube. A 12-sec pulse of the agonist was applied at an interval of about 10 min to allow for complete recovery from any desensitization from a previous agonist pulse. Samples shown were obtained from four SR interneurons in each group. **B.** Bar graph showing the mean ± SEM net charge of NMDA EPSCs at each ACh concentration in both groups of rats. The data were obtained from five to 14 neurons at each ACh concentration. Saline and nicotine injections were done by the same protocol as described in figure legend 1. Significant differences between saline and nicotine groups were found by Mann-Whitney test ($p < 0.02$ at 30 μM ACh; $p < 0.01$ at 10 μM, 100 μM and 1000 μM ACh).

Fig. 5. Two in vivo nicotine injections do not affect the number of NMDA receptors or of glutamate synapses. **A**. Samples of outward currents evoked by U-tube application of NMDA (50 μM) plus glycine (10 μM) to CA1 SR interneurons in both groups of animals. The slow rise time in the NMDA-evoked currents can be attributed to the use of a non-saturating agonist concentration as well as to the slow access of the agonist to the receptor sites on the dendritic branches in the slices. Membrane Potential = +40 mV. MLA (10 nM) was included in the ACSF to inhibit Type IA nAChRs. **B.** Samples of outward NMDA EPSCs evoked by U-tube application of 500 mM sucrose in ACSF. Membrane potential = +40 mV. Bath application of

APV (50 μM) for 8 min attenuated the magnitude of sucrose-induced EPSCs. **C.** Bar graph showing the mean and SEM of the net charge of NMDA- or sucrose-evoked currents from both groups of animals. The number of neurons was seven for NMDA and six for sucrose.

Fig. 6. Single *in vivo* nicotine injection enhances expression of functional Type III nAChRs. **A**. Samples of DMPP-evoked NMDA EPSCs recorded from CA1 SR interneurons from saline-injected and nicotine-injected rats. A single injection of saline or nicotine (0.586 mg/kg, s.c.) was given 17 h before the experiments to rats at postnatal day 15. Membrane Potential = +40 mV. MLA (10 nM) was included in the ACSF to inhibit Type IA nAChRs. **B**. Bar graph showing the mean and SEM of the net charge of DMPP-evoked NMDA EPSCs in the two groups. n = 5 for saline and 7 for nicotine. * $p < 0.02$ by Mann-Whitney test.

Fig. 7. Single *in vivo* nicotine injection does not alter pharmacological properties of Type III nAChRs. **A.** Samples of ACh (0.1 mM)-evoked NMDA EPSCs from a CA1 SR interneuron from nicotine-injected rat. The left trace is the control and the right trace is the response after a 10-min exposure of the slice to 1 μM mecamylamine. **B.** Samples of ACh (0.1 mM)-evoked NMDA EPSCs from another CA1 SR interneuron from nicotine-injected rat. The left trace is the control and the right trace is the response after a 10-min exposure of the slice to 50 nM MLA. A single injection of nicotine (0.586 mg/kg, s.c.) was given 17 h before the experiments to rats at postnatal day 15. Membrane Potential = +40 mV. **C.** Bar graph showing the mean and SEM of the response remaining after exposure of the slices to the antagonists in control and nicotine-injected rats. N = 6 for each group. The net charge of ACh-evoked NMDA EPSCs before

exposure to the antagonist was taken as 100%. The inhibition produced by both antagonists was found to be statistically significant ($p < 0.03$ by Wilcoxon Signed Rank Test). However, no significant differences were found between control and nicotine groups ($p > 0.25$ by Mann Whitney test).

Fig. 8. Acute in vitro exposure to nicotine causes differential desensitization of three nAChR responses in hippocampal slices. **A.** Samples of nicotinic responses representing three nAChR subtypes in hippocampal slices. Top trace in each panel was obtained before exposure to nicotine and bottom trace after 10 min exposure to 100 nM nicotine. Hippocampal slices were obtained from 16- to 19-day-old rats without any pretreatment. Membrane potential = +40 mV, -68 mV, and -68 mV for the three panels from left to right. Recordings were obtained from SR interneurons (for Type IA and Type III responses) and SLM interneuron (for Type II response). **B.** Plots of normalized nicotinic responses. For Type IA nAChRs, the peak amplitude of choline (10 mM)-evoked currents recorded from SR interneurons at -68 mV in the absence of nicotine was taken as 100% and the peak amplitudes of the currents recorded after exposure to different nicotine concentrations were normalized accordingly. Data for Type IA nAChRs was taken from a previous study (Alkondon *et al*, 2000). For Type II nAChRs, the net charge of slow nicotinic currents activated by ACh (0.1 mM in the presence of 10 nM MLA) recorded from SLM interneurons at -68 mV in the absence of nicotine was taken as 100% and the net charge of nicotinic currents recorded after exposure to different concentrations of nicotine were normalized accordingly. For Type III nAChRs, the net charge of ACh (0.1 mM in the presence of 10 nM MLA)-evoked NMDA EPSCs recorded from SR interneurons at +40 mV in the absence of

nicotine was taken as 100% and the net charge of the EPSCs after exposure to different concentration of nicotine were normalized accordingly. Each symbol and error bar represents mean ± SEM values obtained from four to six neurons. The solid line connecting the symbols was derived by fitting the data to a Hill equation. The arterial range in the figure represents the range of human arterial blood nicotine concentrations achieved after smoking a single cigarette (see text for details). The venous range represents the human venous blood nicotine concentrations achieved after smoking several cigarettes.

Fig. 9. Bupropion inhibits potently native Type III nAChRs. **A**. Sample recordings of ACh-induced NMDA EPSCs at +40 mV from a SR interneuron under control and after 10 min bath application of bupropion (1 μM). **B.** Sample recordings of ACh-induced slow-decaying nicotinic currents at -68 mV from a SLM interneuron under control and after 10 min bath application of bupropion (1 μM). **C**. Sample recordings of choline-induced nicotinic currents at -68 mV from a SR interneuron under control and after 10 min bath application of bupropion (1 μM). **D**. Samples of NMDA-evoked currents at +40 mV from a SR interneuron under control and after 10 min bath application of bupropion (1 μM). Bupropion was present in the U-tube and bath solution in all the above experiments. **E**. Average values (mean ± SEM) of each response in the presence of 1 μM bupropion from several neurons. The percent response in the presence of bupropion in each neuron was calculated based on the control and the wash responses. N = 6 for ACh-induced NMDA EPSCs, and 4 for all the others. * $p < 0.05$; ** $p < 0.01$ by paired '*t*' test.

JPET Fast Forward. Published on January 12, 2005 as DOI: 10.1124/jpet.104.081232
This article has not been copyedited and formatted. The final version may differ from this version.

Table 1: Analysis of ACh-evoked Type II currents in CA1 SLM interneurons

Treatment	Peak Amplitude Analysis			Net Charge Analysis		
	EC50 (μM)	Hill coefficient	Maximum amplitude	EC50 (μM)	Hill coefficient	Maximum Charge
Saline	112 ± 24	1.07 ± 0.22	54.2 ± 13.5	117 ± 22	1.03 ± 0.18	476 ± 98
Nicotine	123 ± 33	0.83 ± 0.18	105 ± 9.4[a]	104 ± 28	1.00 ± 0.26	979 ± 107[a]

Two subcutaneous injections of saline or nicotine were administered to rats as described in the Methods section.

[a] $p < 0.02$ compared to saline group by Mann-Whitney U-test.

JPET Fast Forward. Published on January 12, 2005 as DOI: 10.1124/jpet.104.081232
This article has not been copyedited and formatted. The final version may differ from this version.

Table 2: Characteristics of AMPA EPSCs recorded from CA1 SR interneurons

Parameter	Saline	N	Nicotine	N
Frequency (Hz)				
Spontaneous	0.047 ± 0.012	14	0.084 ± 0.019	18
ACh (10 μM)	0.062 ± 0.025	8	0.278 ± 0.075[b,d]	8
ACh (100 μM)	0.218 ± 0.049[a]	8	1.052 ± 0.201[c,e]	9
Peak Amplitude (pA)				
Spontaneous	16.2 ± 1.4	13	15.9 ± 0.8	18
ACh (10 μM)	15.2 ± 1.0	7	16.2 ± 0.9	7
ACh (100 μM)	19.0 ± 1.9	7	24.2 ± 2.8[f]	7
Rise Time (ms)				
Spontaneous	0.85 ± 0.08	13	1.08 ± 0.13	17
ACh (10 μM)	0.85 ± 0.11	7	1.11 ± 0.16	7
ACh (100 μM)	0.98 ± 0.21	7	0.97 ± 0.08	7
Decay-Time Constant (ms)				
Spontaneous	3.33 ± 0.40	13	3.95 ± 0.44	16
ACh (10 μM)	3.51 ± 0.37	7	4.00 ± 0.39	7
ACh (100 μM)	3.12 ± 0.36	7	3.07 ± 0.25	7

Two subcutaneous injections of saline or nicotine were administered to rats as described in the Methods section.

All the following comparisons were done by Mann-Whitney U-test.

N = number of neurons.
[a] $p < 0.001$ compared to spontaneous frequency in saline group.
[b] $p < 0.01$ compared to spontaneous frequency in nicotine group.
[c] $p < 0.0001$ compared to spontaneous frequency in nicotine group.
[d] $p < 0.005$ compared to ACh (10 μM) in saline group.
[e] $p < 0.002$ compared to ACh (100 μM) in saline group.
[f] $p < 0.001$ compared to spontaneous peak amplitude in nicotine group.

JPET Fast Forward. Published on January 12, 2005 as DOI: 10.1124/jpet.104.081232
This article has not been copyedited and formatted. The final version may differ from this version.

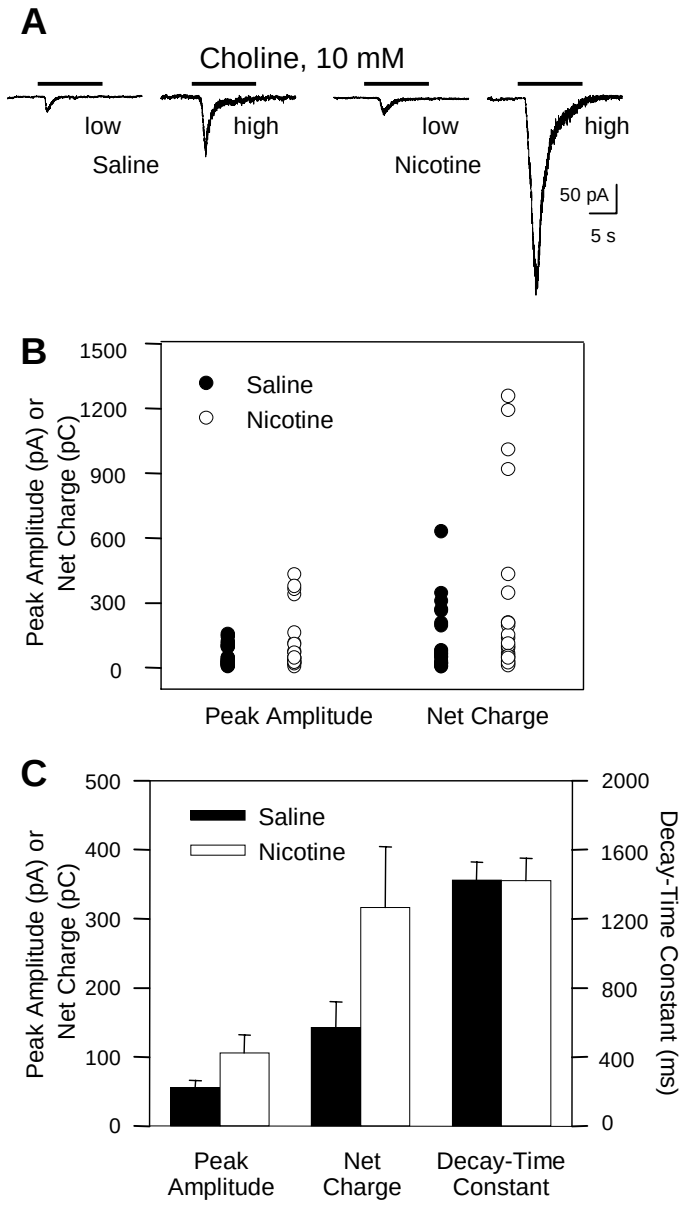

FIGURE 1

JPET Fast Forward. Published on January 12, 2005 as DOI: 10.1124/jpet.104.081232
This article has not been copyedited and formatted. The final version may differ from this version.

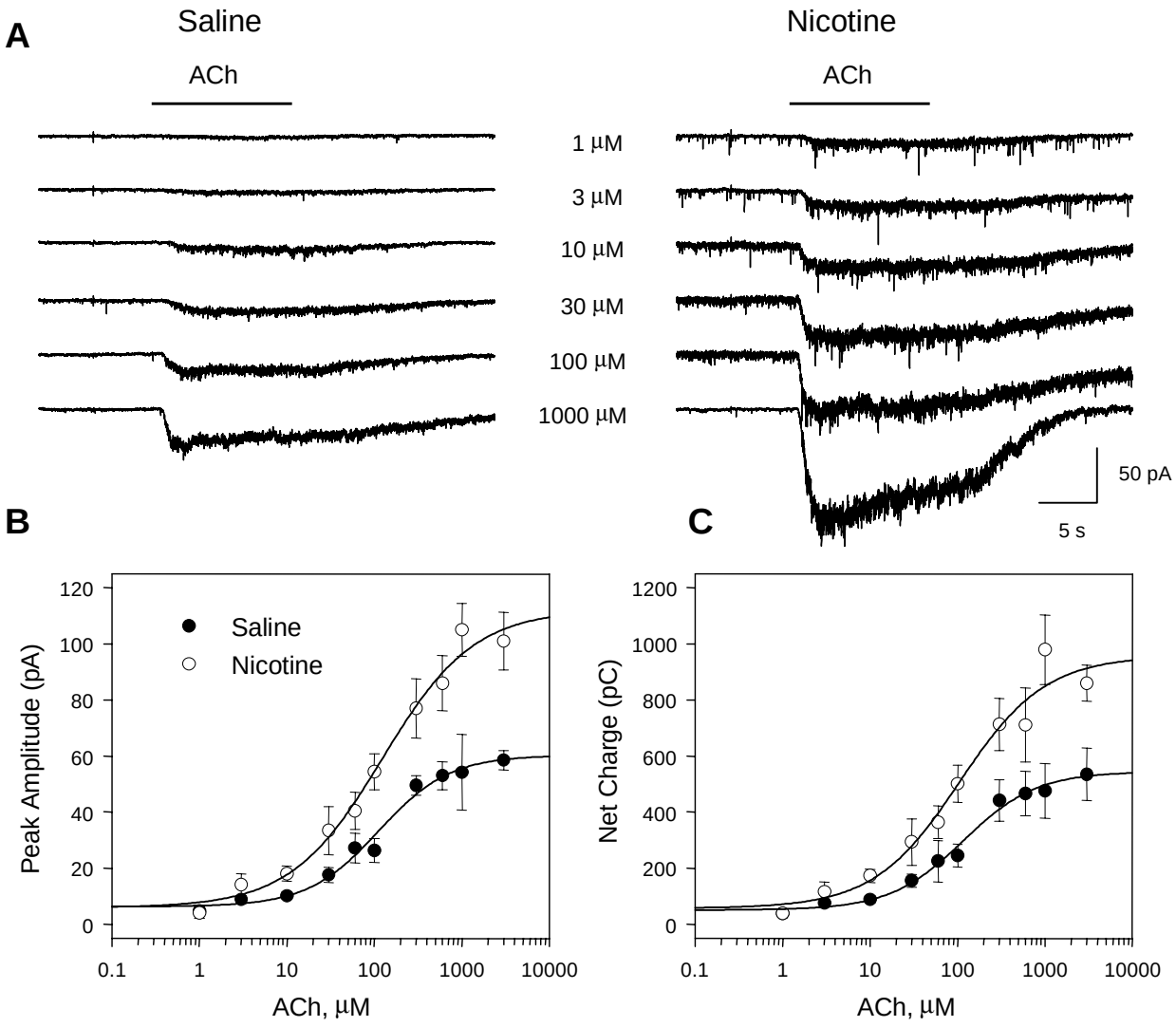

FIGURE 2

JPET Fast Forward. Published on January 12, 2005 as DOI: 10.1124/jpet.104.081232
This article has not been copyedited and formatted. The final version may differ from this version.

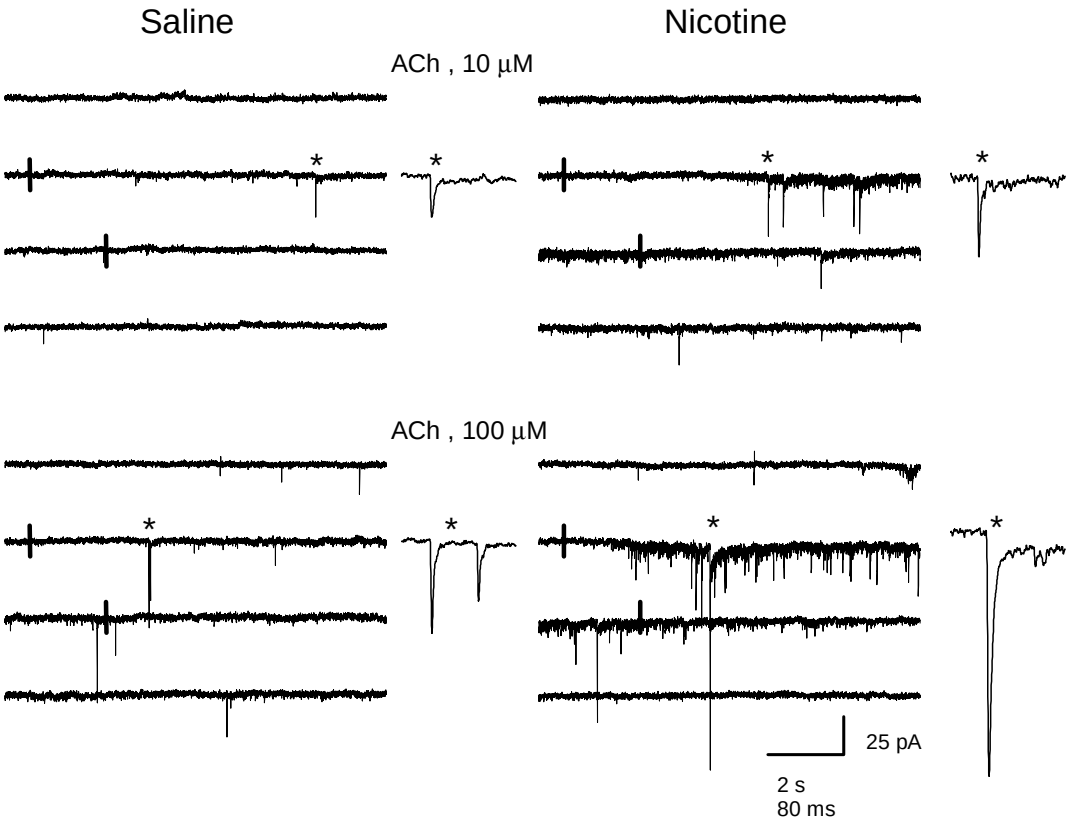

FIGURE 3

JPET Fast Forward. Published on January 12, 2005 as DOI: 10.1124/jpet.104.081232
This article has not been copyedited and formatted. The final version may differ from this version.

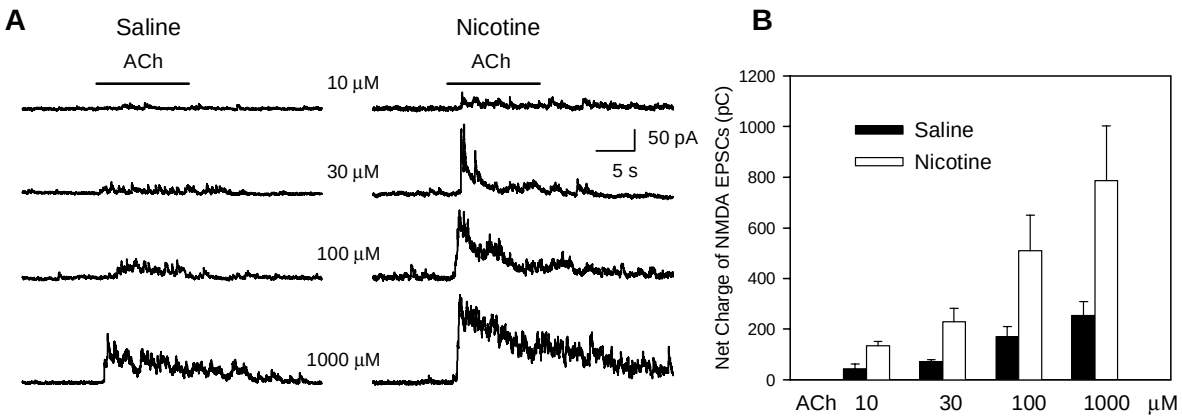

FIGURE 4

JPET Fast Forward. Published on January 12, 2005 as DOI: 10.1124/jpet.104.081232
This article has not been copyedited and formatted. The final version may differ from this version.

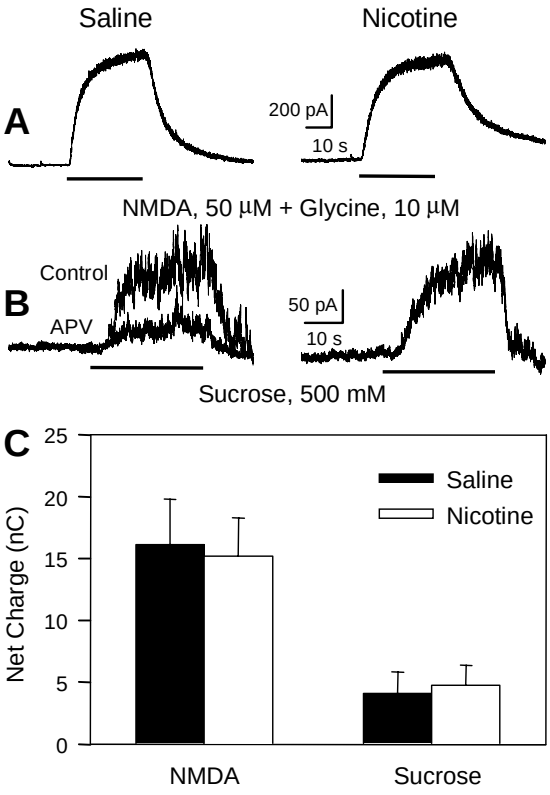

FIGURE 5

JPET Fast Forward. Published on January 12, 2005 as DOI: 10.1124/jpet.104.081232
This article has not been copyedited and formatted. The final version may differ from this version.

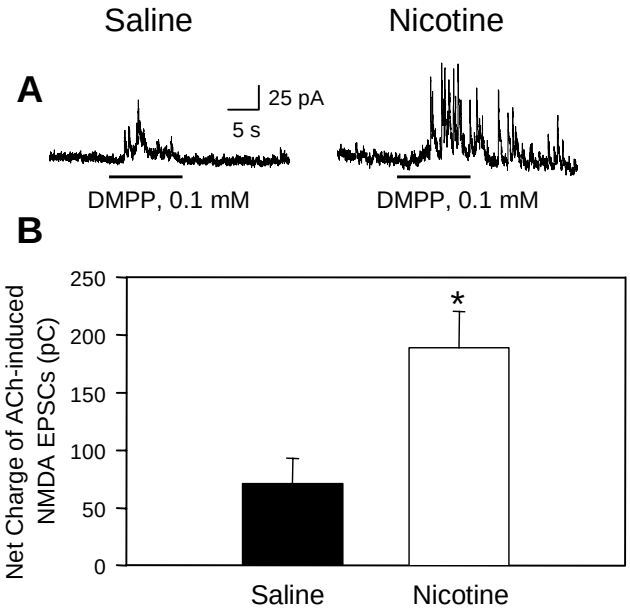

FIGURE 6

JPET Fast Forward. Published on January 12, 2005 as DOI: 10.1124/jpet.104.081232
This article has not been copyedited and formatted. The final version may differ from this version.

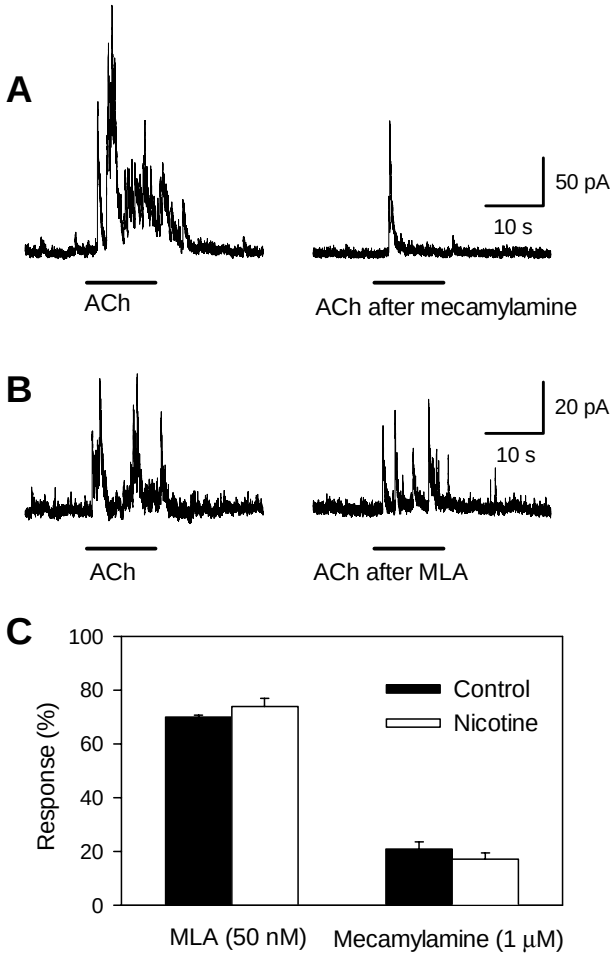

FIGURE 7

JPET Fast Forward. Published on January 12, 2005 as DOI: 10.1124/jpet.104.081232
This article has not been copyedited and formatted. The final version may differ from this version.

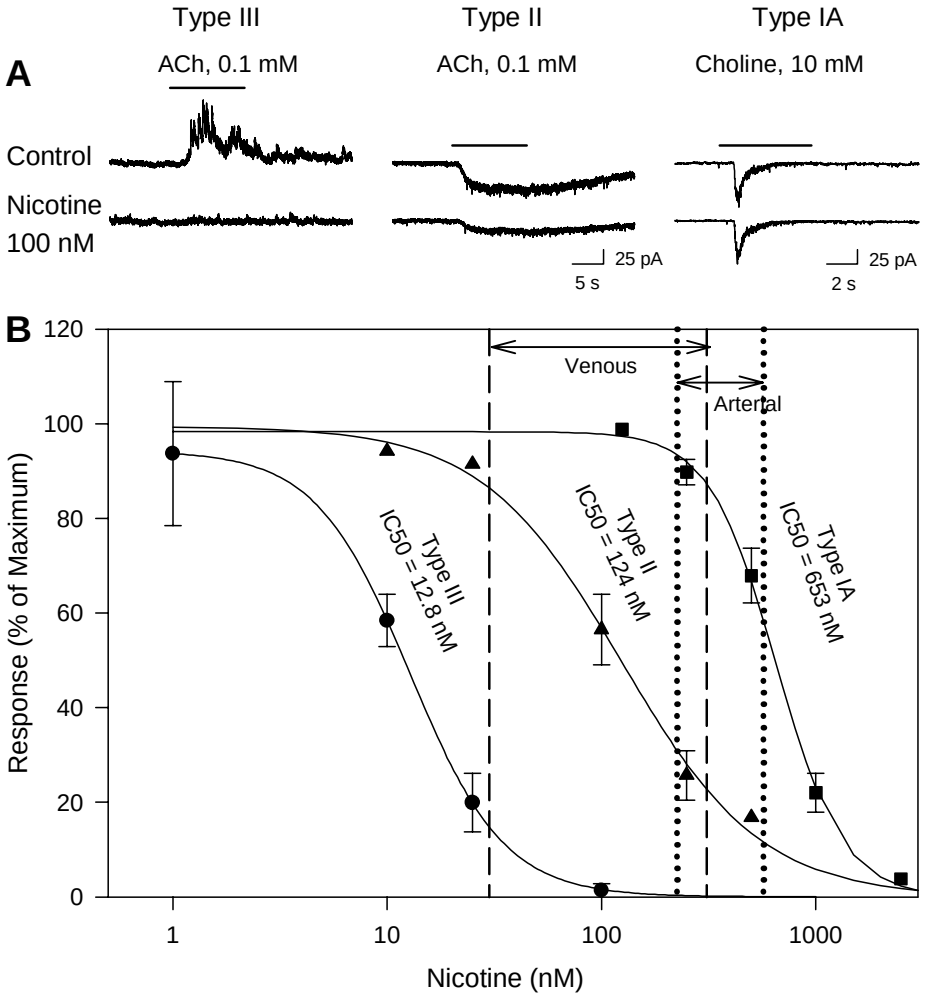

FIGURE 8

JPET Fast Forward. Published on January 12, 2005 as DOI: 10.1124/jpet.104.081232
This article has not been copyedited and formatted. The final version may differ from this version.

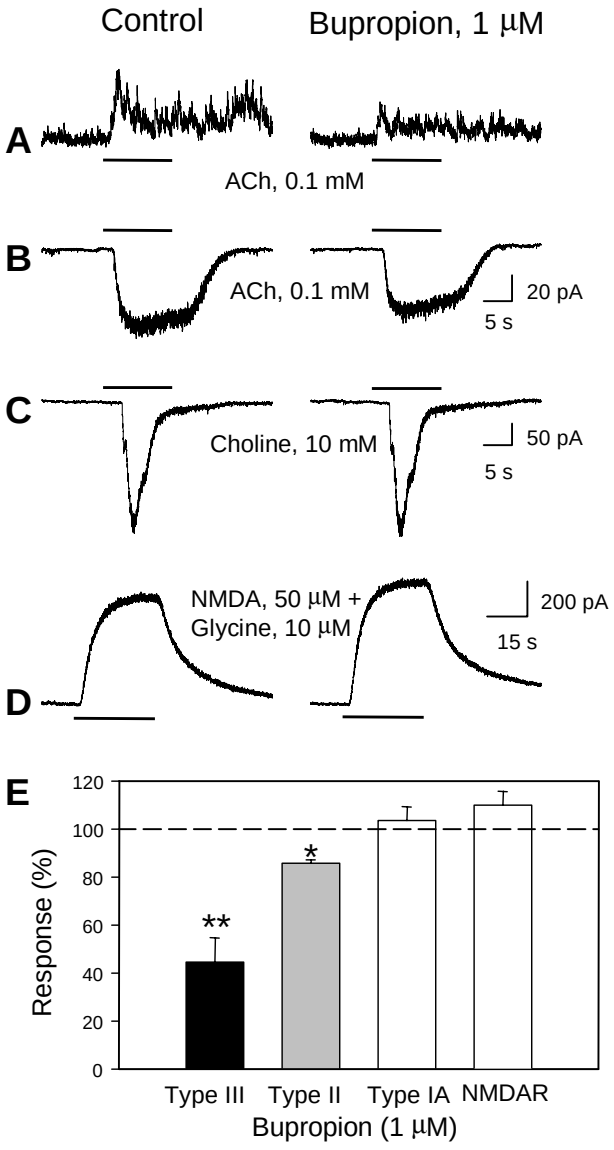

FIGURE 9